

Carbonated Hydroxyapatite (CHAp)/PCL/Gelatin Scaffold Synthesized from Wrinkled Purple Snail Shell Waste for Bone Regeneration

Fadilah Salsabilla, Rosita Wati*, Aldi Herbanu, Marsudi Siburian, and Endah

Department of Biomedical Engineering, Institut Teknologi Sumatera, Lampung Selatan, Indonesia, 35365

Article Information

Article history:

Received September 2, 2025
Received in revised form October 28, 2025
Accepted October 29, 2025

Keywords: wrinkled purple snail, freeze-drying, carbonate hydroxyapatite, polycaprolactone, scaffold

Abstract

Traffic accidents are a major cause of bone fractures in Indonesia, highlighting the urgent need for effective biomaterials in bone regeneration. This study synthesized carbonated hydroxyapatite (CHAp) from wrinkled purple sea snail shells (*Nucella lamellosa*) using a precipitation method and sintering at 600 °C, followed by the fabrication of CHAp/PCL/Gelatin scaffolds through freeze-drying. XRD confirmed B-type CHAp with a crystallite size of 9.86 nm, crystallinity of 62.07%, and a Ca/P ratio of 1.76. The incorporation of PCL and gelatin decreased scaffold crystallinity to 37.29% and increased the Ca/P ratio to 3.19. FTIR spectra verified the presence of CO_3^{2-} , PO_4^{3-} , OH^- groups, as well as characteristic peaks of PCL and gelatin. SEM analysis revealed a porous interconnected structure with an average pore size of 28.94 μm . The scaffold exhibited compressive strength of 2.693 MPa, within the range of trabecular bone, and showed a 3% mass loss after 24 h, indicating suitable initial biodegradation. These findings demonstrate the potential of snail shell-derived CHAp/PCL/Gelatin scaffolds as biodegradable biomaterials for bone regeneration.

Informasi Artikel

Proses artikel:

Diterima 2 September 2025
Diterima dan direvisi dari 28 Oktober 2025
Accepted 29 Oktober 2025

Kata kunci: keong ungu keriput, freeze-drying, karbonat hidroksiapatit, polikaprolakton, scaffold

Abstrak

Kecelakaan lalu lintas merupakan penyebab utama patah tulang di Indonesia, sehingga diperlukan biomaterial yang efektif untuk regenerasi tulang. Penelitian ini bertujuan untuk mensintesis karbonat hidroksiapatit (CHAp) dari cangkang keong laut ungu keriput (*Nucella lamellosa*) menggunakan metode presipitasi dan sintering pada suhu 600 °C, kemudian dilanjutkan dengan pembuatan scaffold CHAp/PCL/Gelatin melalui metode freeze-drying. Hasil XRD mengonfirmasi bahwa CHAp yang terbentuk merupakan tipe B dengan ukuran kristalit 9.86 nm, tingkat kristalinitas 62.07%, dan rasio Ca/P sebesar 1.76. Penambahan PCL dan gelatin menurunkan kristalinitas scaffold menjadi 37.29% dan meningkatkan rasio Ca/P menjadi 3.19. Analisis FTIR menunjukkan keberadaan gugus fungsi CO_3^{2-} , PO_4^{3-} , dan OH^- , serta puncak khas dari PCL dan gelatin. Analisis SEM memperlihatkan struktur berpori dengan keterhubungan yang baik dan rata-rata ukuran pori 28.94 μm . Uji mekanik menunjukkan kekuatan tekan scaffold sebesar 2.693 MPa, berada dalam rentang nilai kekuatan tulang trabekular, sementara uji biodegradasi menunjukkan kehilangan massa sebesar 3% setelah 24 jam, yang menandakan laju degradasi awal yang sesuai. Hasil ini menunjukkan bahwa scaffold CHAp/PCL/Gelatin berbasis limbah cangkang keong memiliki potensi sebagai biomaterial biodegradable untuk aplikasi regenerasi tulang.

* Corresponding author.

E-mail address: rosita.wati@bm.itera.ac.id

1. Introduction

Traffic accidents are among the leading causes of bone fractures in Indonesia, often resulting in disabilities that require advanced medical interventions. According to the World Health Organization (WHO), millions of bone injury cases, including those caused by traffic accidents, occur worldwide each year. In Indonesia, the Ministry of Health reported that traffic accidents are one of the main contributors to bone injuries, with the 2018 Riskesdas survey showing that 31.4% of injuries occur on the road, 44.7% in the home environment, and 9.1% in the workplace (Kementerian Kesehatan RI, 2018). Bone fractures demand effective treatments, and one promising approach is bone tissue engineering (Cieza, A., et al., 2021).

Bone tissue engineering integrates biological science and engineering to restore, repair, or maintain damaged tissue function. Scaffolds play a crucial role as three-dimensional (3D) structures that support cell attachment, proliferation, and differentiation, facilitating tissue regeneration (Lee et al., 2022). The choice of biomaterial is critical to scaffold performance, particularly for bone tissue engineering. Among various biomaterials, calcium phosphate-based bioceramics, such as hydroxyapatite (HAp) and its carbonate-substituted form, carbonated hydroxyapatite (CHAp), are widely used due to their biocompatibility, bioactivity, and osteoconductivity (Min et al., 2024).

Bone tissue damage remains a major health concern in Indonesia due to high cases of accidents and degenerative bone diseases, leading to an increased need for effective bone regeneration strategies. However, conventional bone grafts often face limitations such as donor site morbidity, infection risk, and high cost. Therefore, the development of biocompatible, biodegradable, and sustainable scaffolds for bone tissue engineering is urgently needed. This research focuses on synthesizing Carbonated Hydroxyapatite (CHAp) derived from *Wrinkled Purple Snail Shells*, combined with PCL and gelatin, to provide an eco-friendly and effective alternative scaffold for bone regeneration applications.

In this study, CHAp was synthesized from *wrinkled purple snail shell* (*Nucella lamellose*), an abundant marine waste in coastal Lampung (Permatasari et al., 2021). The synthesis of CHAp from *wrinkled purple snail shells* aligns with green synthesis principles because it utilizes marine waste as a calcium source, minimizes the use of hazardous chemicals, and promotes resource sustainability (Nguyen et al., 2022). This eco-friendly approach supports the concept of sustainable biomaterial development in biomedical engineering. The physicochemical, mechanical, and biodegradation properties to assess its potential for bone tissue engineering application

2. Research Methods

2.1 Tools and Materials

The tools used in this research included an analytical (for accurate weighing), an oven (for drying samples), a furnace (for sintering), a magnetic stirrer (for homogeneous mixing), a centrifuge (for separating precipitate), and a freeze dryer (for obtaining porous structures). Characterization instruments consisted of X-ray Diffraction (XRD, to determine crystal phases), Fourier Transform Infrared Spectroscopy (FTIR, to identify functional groups), Scanning Electron Microscope–Energy Dispersive X-ray (SEM–EDX, to observe morphology and elemental composition), and Universal Testing Machine (UTM, to evaluate mechanical strength). The materials used were wrinkled purple snail shells (*Nucella lamellose*), collected from coastal areas in Lampung, Indonesia; sodium hydroxide (NaOH, Merck, $\geq 99\%$ purity); ammonium dihydrogen phosphate ($\text{NH}_4\text{H}_2\text{PO}_4$, Merck, analytical grade); polycaprolactone (PCL, Sigma-Aldrich, Mw 80,000); and gelatin (food grade). Distilled water was used as a solvent throughout the synthesis process.

2.2 Preparation of Raw Wrinkled Purple Snail Shell

The raw shells of wrinkled purple sea snails (*Nucella lamellose*) were collected from coastal areas in Lampung, Indonesia. Prior to use, the shells were thoroughly cleaned by boiling in distilled water for 30 minutes to remove organic debris and surface impurities. The cleaned shells were then dried under the sun for 24 hours, followed by oven drying at 100°C for 2 hours to eliminate residual moisture. After drying, the shells were mechanically crushed into smaller fragments using a mortar and pestle and further ground into fine powder with a ball mill. The powdered shells served as the calcium source for the subsequent synthesis of carbonated hydroxyapatite (**Figure 1**).

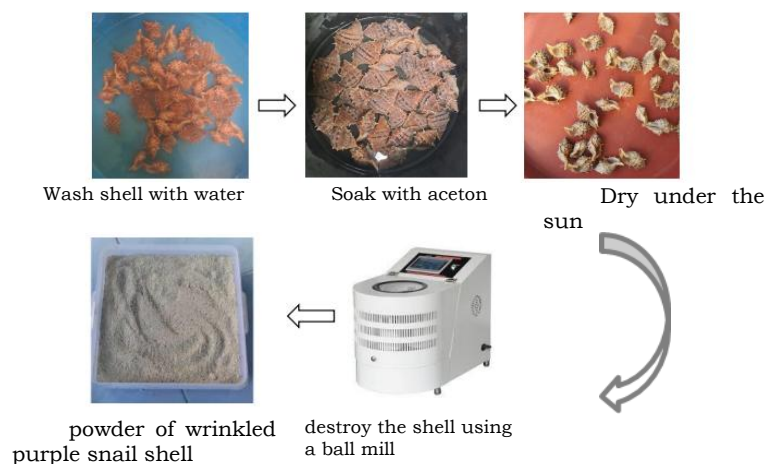


Figure 1. Preparation step

2.3 Synthesis of CHAp

Wrinkled purple snail shells were washed, boiled, and dried to remove organic residues. The dried shells were calcined at 1000 °C for 4 hours to obtain CaO powder. CaO was then dissolved in distilled water to form Ca(OH)₂ solution. NH₄H₂PO₄ solution was prepared separately. The Ca(OH)₂ solution was added dropwise with NH₄H₂PO₄ under continuous stirring at a Ca/P molar ratio of 1.67 (corresponding to a molar ratio of Ca : P : C = 0.4175 : 0.25 : 0.25), maintaining pH 10 by adding NaOH 1 M. The precipitate was aged for 24 hours, filtered, and dried at 100 °C. The powder was sintered at 600 °C for 2 hours to obtain CHAp (**Figure 2**).

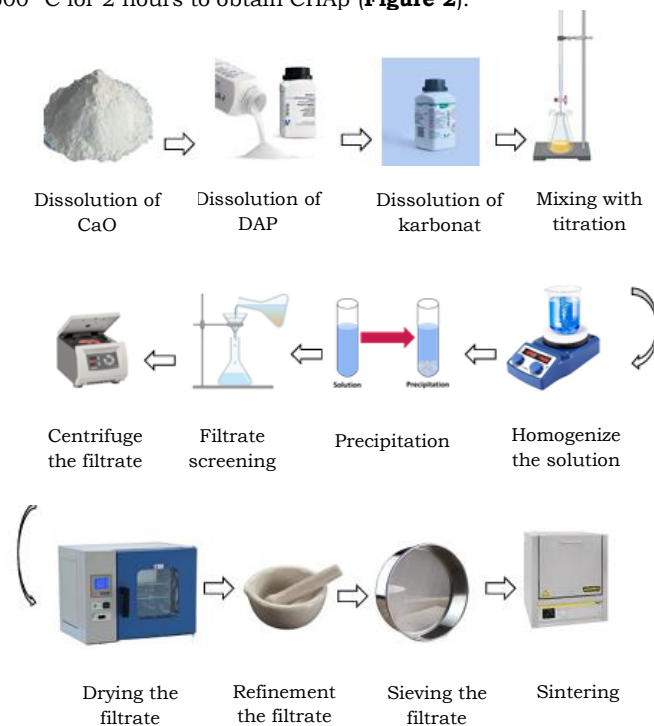


Figure 2. Synthesis of CHAp

2.4 Fabrication of CHAp/PCL/Gelatin Scaffold

PCL was dissolved in dichloromethane (DCM) and mixed with gelatin dissolved in distilled water at 50 °C, using a composition of 3 g CHAp in 30 mL solvent (0.1 M), 1.8 g PCL in 18 mL acetone (1.25×10^{-3} M), and 2.6 g gelatin in 26 mL solvent (1.1×10^{-3} M). CHAp powder was gradually added to the polymer solution and stirred until homogeneous. The suspension was poured into molds and frozen at -20 °C for 24 hours, followed by freeze-drying for 48 hours to produce porous CHAp/PCL/Gelatin scaffold (**Figure 3**).

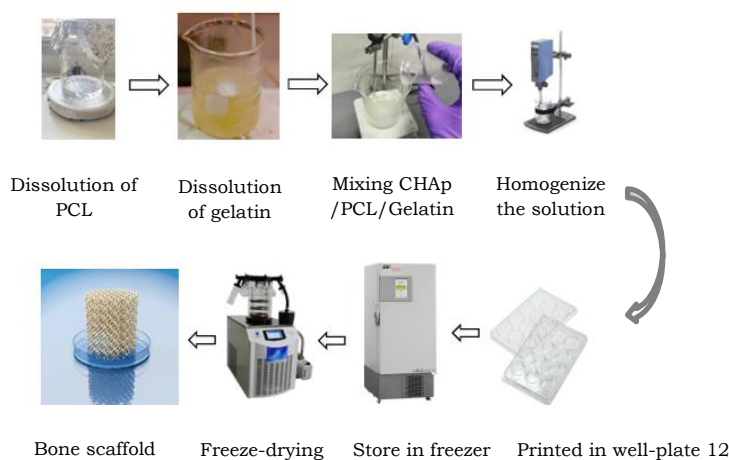


Figure 3. Fabrication of Scaffold CHAp/PCL/Gelatin

2.5 Characterization

The CHAp powder and CHAp/PCL/Gelatin scaffolds were characterized using several analytical techniques. X-ray diffraction (XRD) was employed to identify crystalline phases, calculate crystallite size using the Scherrer equation, and determine the crystallinity index. In addition, CaO obtained from calcined snail shells was also characterized using XRD to confirm the successful phase transformation from CaCO_3 to CaO. Fourier transform infrared spectroscopy (FTIR) was used to confirm the presence of functional groups such as CO_3^{2-} , PO_4^{3-} , and OH^- , as well as polymer-specific peaks from PCL and gelatin. The surface morphology and pore structure were observed using scanning electron microscopy (SEM) coupled with energy dispersive X-ray spectroscopy (EDX) for elemental composition analysis. The compressive strength of the scaffolds was measured using a universal testing machine (UTM) and calculated from the ratio between the maximum applied load and the cross-sectional area. Biodegradation testing was performed by immersing the scaffolds in phosphate-buffered saline (PBS) at 37 °C for 24 hours, after which the weight loss percentage was determined to evaluate the initial degradation rate.

3. Results and Discussions

3.1 Characterization of Calcium Oxide (CaO) Powder from Wrinkled Purple Snail Shell

The crystalline structure of the obtained CaO powder was characterized using X-ray diffraction (XRD) to confirm its phase composition. As shown in **Figure 4**, the XRD pattern of the CaO sample exhibited characteristic diffraction peaks that matched well with the standard reference data of JCPDS CaO No. 37-1497, indicating the successful formation of calcium oxide. This step was performed to confirm the presence of calcium content, which is essential for bone tissue engineering applications. The presence of these diffraction peaks confirmed that the calcination process at 900 °C for 5 hours effectively removed organic components and transformed calcium carbonate (CaCO_3) from the snail shells into calcium oxide (CaO). This result verifies that the raw material contained a sufficient amount of calcium oxide, thus fulfilling the prerequisite for CHAp synthesis. This finding is consistent with Rahman et al. (2021), who reported that seashell-derived CaO exhibited similar dominant peaks at $2\theta \approx 32\text{--}37^\circ$, confirming high crystallinity after calcination at 900–1000 °C. Likewise, Zhang et al. (2020) also observed comparable CaO peaks from biogenic precursors, demonstrating that marine-shell-derived CaO consistently produces phase-pure and crystalline oxide suitable for biomaterial applications.

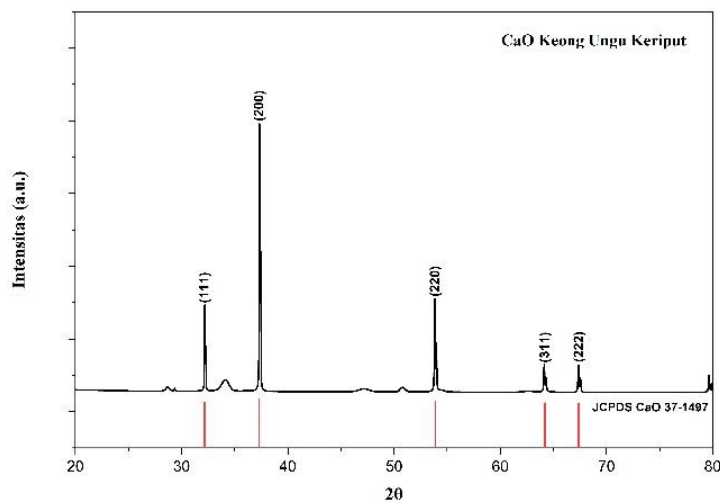


Figure 4. XRD patterns of CaO powder

3.2 Characterization of Carbonated Hydroxyapatite (CHAp)

1. X-ray diffraction (XRD) Analysis. The XRD pattern of CHAp synthesized from *Nucella lamellosa* shells in **Figure 5** showed characteristic peaks corresponding to carbonated hydroxyapatite (B-type), with major reflections at 2θ values of approximately 25.9°, 31.8°, and 32.9° (JCPDS 09-0432). The absence of the (112) peak indicated partial substitution of PO_4^{3-} by CO_3^{2-} ions, consistent with B-type carbonate substitution ((Figueiredo et al., 2021). This substitution is beneficial as it improves solubility and bioactivity, making the phase more similar to natural bone apatite.

The lattice parameters obtained from refinement were $a = b = 9.36 \text{ \AA}$ and $c = 6.87 \text{ \AA}$, which are in agreement with standard values of carbonated hydroxyapatite. The calculated crystallite size using the Scherrer equation was **9.86 nm**, confirming the nanocrystalline nature of the material. Additionally, the estimated microstrain was **0.0124**, indicating slight lattice distortions, which are typical for carbonate-substituted hydroxyapatite due to ionic substitution within the crystal structure. The crystallinity index was 62.07% further confirming that the CHAp retained a partially ordered crystalline phase. This conclusion was drawn from the presence of sharp and well-defined diffraction peaks with low background noise, indicating long-range atomic ordering typical of crystalline

hydroxyapatite. In contrast, amorphous phases would exhibit broad and diffuse peaks; therefore, the XRD pattern verified that the carbonation process did not disrupt the fundamental HA crystalline structure (Li, Y., et al., 2021).

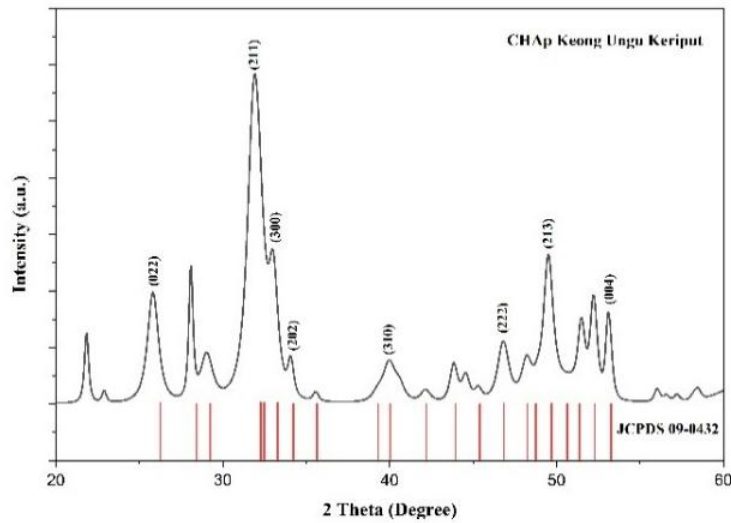


Figure 5. XRD patterns of CHAp powder

Such nanoscale crystallinity and slight lattice distortion are advantageous for biomedical applications, as they enhance protein adsorption, promote bioactivity, and support osteoblast adhesion and proliferation (Ebrahimi et al., 2022). The obtained crystallite size of 10 nm is within the biologically relevant range of bone apatite, reinforcing the potential of CHAp derived from *Nucella lamellosa* as a bone substitute material.

2. Fourier Transform Infrared (FTIR) Analysis. The FTIR spectrum of the synthesized CHAp revealed several absorption bands characteristic of functional groups typically present in carbonated hydroxyapatite. Strong absorption bands of PO_4^{3-} were observed at 1034 cm^{-1} (ν_3), 962 cm^{-1} (ν_1), and 566 cm^{-1} (ν_4), which correspond to the vibrational modes of phosphate groups and confirm the successful incorporation of phosphate into the CHAp lattice. In addition, CO_3^{2-} absorption bands were identified at 1416 cm^{-1} and 871 cm^{-1} , indicating carbonate substitution into the apatite structure. The OH^- stretching vibration was detected at 3570 cm^{-1} , further supporting the formation of hydroxyapatite. As shown in **Figure 6**, the FTIR spectrum clearly demonstrates that the material obtained is B-type carbonated hydroxyapatite (B-type CHAp), where carbonate groups substitute for phosphate sites. This substitution pattern is particularly important because B-type CHAp is known to closely resemble the composition of biological apatite found in natural bone. These observations are consistent with previous findings reported in the literature (Sun et al., 2022). The FTIR results, when correlated with the XRD analysis, confirm the successful synthesis of B-type CHAp with both phosphate and carbonate groups present, suggesting that the biomaterial has high potential for bone tissue engineering applications due to its similarity with natural bone mineral. This agreement between FTIR and XRD results indicates successful incorporation of carbonate into the apatite lattice (Martins et al., 2023). Therefore, both analyses confirm the formation of B-type carbonated hydroxyapatite with lattice substitution similar to natural bone mineral, reinforcing its potential for bone tissue engineering applications.

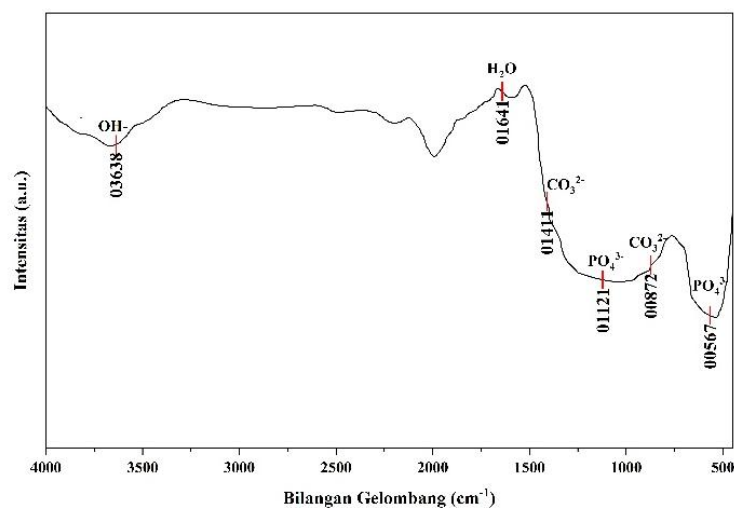


Figure 6. FTIR spectra of CHAp powder

3. *Scanning Electron Microscopy–Energy Dispersive X-ray (SEM-EDX) Analysis.* The SEM micrograph of CHAp powder in **Figure 7** shows irregularly shaped particles with a rough and porous surface, which is typical of nanocrystalline hydroxyapatite morphology. The porous surface provides a high surface area, which is beneficial for facilitating protein adsorption and enhancing osteoblast attachment during bone tissue regeneration. The presence of nanosized particles is also advantageous since nanostructured hydroxyapatite has been reported to mimic the mineral phase of natural bone more closely, thereby improving its bioactivity and biocompatibility (Ielo et al., 2022).

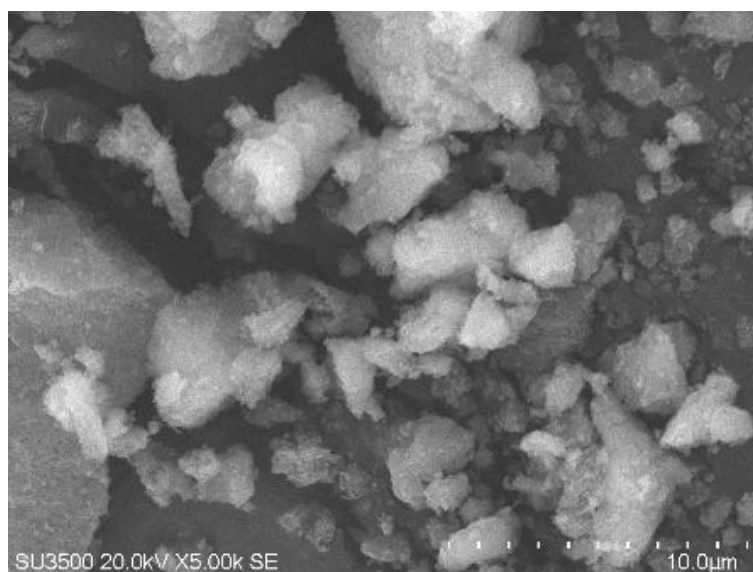


Figure 7. SEM micrographs of CHAp powder

EDX analysis of CHAp confirmed the presence of calcium (Ca), phosphorus (P), oxygen (O), and carbon (C), consistent with the composition of B-type carbonated hydroxyapatite. The corresponding atom concentrations are shown in **Table 1**. The calculated Ca/P atomic ratio of 1.76 is close to the theoretical value of 1.67 for natural bone mineral. This result agrees with the FTIR findings and verifies the successful formation of B-type CHAp with carbonate substitution.

Table 1. Elemental Composition of CHAp Powder Based on EDX Analysis

Element	Weight %	Atomic %
Ca	62.04	47.52
P	21.06	20.75
O	16.29	31.08
C	0.25	0.64

3.3 Characterization of CHAp/PCL/Gelatin Scaffold

1. *X-ray diffraction (XRD) Analysis.* The XRD profile of the CHAp/PCL/Gelatin scaffold in **Figure 8** exhibited a significant reduction in crystallinity due to the incorporation of amorphous polymers, which masked several characteristic CHAp diffraction peaks. The XRD profile of the CHAp/PCL/Gelatin scaffold in **Figure 8** exhibited a significant reduction in crystallinity (37.29%) due to the incorporation of amorphous polymers (PCL and gelatin), which masked several CHAp diffraction peaks. The peak broadening and intensity reduction indicate strong polymer–ceramic interactions. This decrease in crystallinity is commonly reported in composite scaffolds and is advantageous in bone tissue engineering because lower crystallinity accelerates degradation and enhances ion release for osteogenesis (Liu et al., 2022).

Additionally, the amorphous nature of the composite scaffold provides better flexibility and degradation control, while still maintaining the bioactivity of CHAp. The broader diffraction peaks observed in the scaffold compared to the sharper peaks of CHAp powder indicate that the polymers effectively disrupted the long-range order of CHAp, thereby producing a composite material with tunable physicochemical properties (Todd et al., 2024). Thus, the combination of CHAp with PCL and gelatin results in a scaffold that not only maintains the bioactive mineral phase but also benefits from enhanced processability and favorable degradation kinetics for bone tissue regeneration applications.

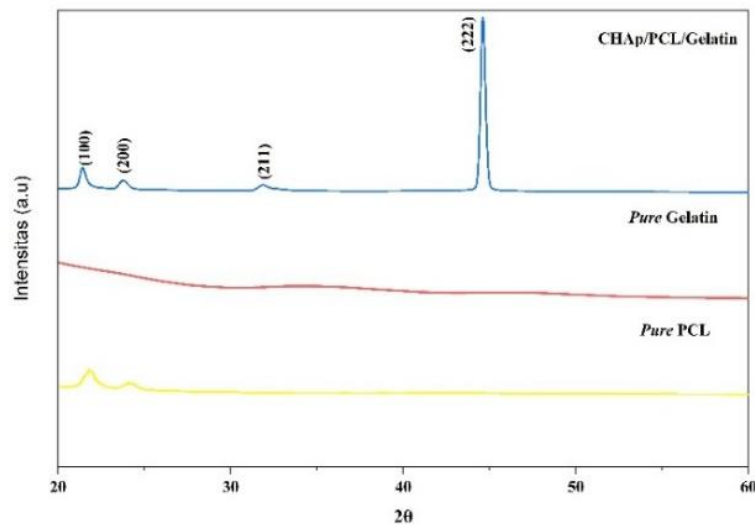


Figure 8. XRD patterns of CHAp/PCL/Gelatin Scaffold

2. *Fourier Transform Infrared (FTIR) Analysis.* The FTIR spectrum of the CHAp/PCL/Gelatin scaffold exhibited not only the characteristic bands of CHAp but also additional absorption peaks corresponding to the polymer components. For PCL, distinctive bands were identified at 1720 cm^{-1} (C=O stretching) and 2940 cm^{-1} (CH_2 stretching), while gelatin contributed amide I (1640 cm^{-1}), amide II (1540 cm^{-1}), and COO^- (1450 cm^{-1}) bands. As presented in **Figure 9**, these peak assignments are consistent with previous FTIR reports of CHAp/PCL/Gelatin composites, which also exhibited phosphate bands of CHAp, carbonyl and ether peaks of PCL, and amide bands of gelatin (Ahmed et al., 2022). This agreement with the literature confirms that the characteristic chemical structure of each component is preserved in the scaffold. Importantly, the preservation of phosphate, carbonate, and hydroxyl bands of CHAp within the composite demonstrates that the polymer blending process did not degrade or alter the intrinsic chemical structure of the apatite. The coexistence of CHAp and polymer-specific peaks highlights that the scaffold maintains the bioactive properties of CHAp, while the polymeric components provide enhanced flexibility, controlled degradation, and improved handling properties. This dual functionality is particularly advantageous for bone tissue engineering, as it supports both biological performance and mechanical integrity throughout the bone regeneration process (Rahman et al., 2023).

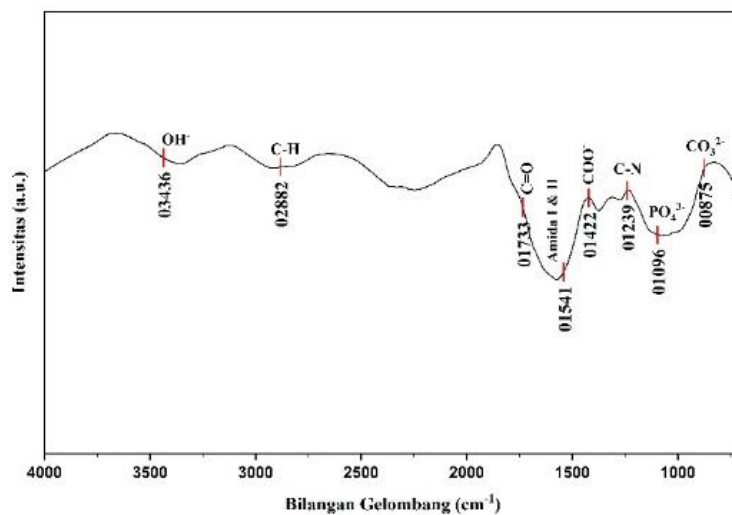


Figure 9. FTIR spectra of CHAp/PCL/Gelatin scaffold

3. *Scanning Electron Microscopy–Energy Dispersive X-ray (SEM-EDX) Analysis.* The CHAp/PCL/Gelatin scaffold in **Figure 10** exhibited a highly porous and interconnected morphology, with an average pore diameter of $28.94\text{ }\mu\text{m}$. This pore size falls within the optimal range for bone tissue engineering ($20\text{--}150\text{ }\mu\text{m}$), which is known to facilitate nutrient and oxygen diffusion, promote vascularization, and support new tissue ingrowth (Hernandez & Woodrow, 2024). The pores appeared relatively uniform and well-distributed, suggesting that the freeze-drying process was

effective in generating an open and interconnected porous network. Such a structure is critical for providing the necessary microenvironment for cell proliferation and differentiation in bone regeneration.

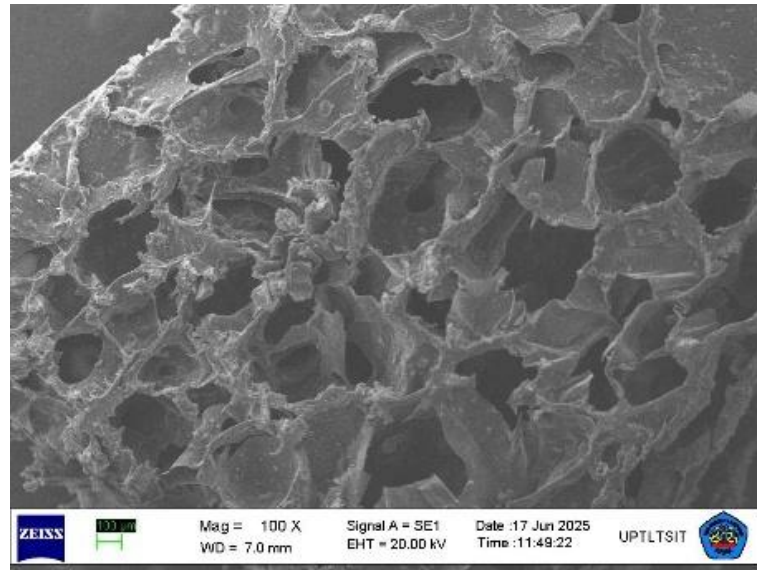


Figure 10. SEM micrographs of CHAp/PCL/Gelatin scaffold

The EDX spectrum of the composite scaffold confirmed the presence of calcium (Ca), phosphorus (p), oxygen (O), and carbon (C), consistent with the mineral phase of B-type carbonated hydroxyapatite as shown in **Table 2**. In addition, additional elemental signals for carbon and nitrogen were detected, which originated from the PCL and gelatin polymers, respectively. This finding confirms the successful incorporation of polymers into the CHAp matrix without eliminating or degrading the mineral phase. The Ca/P molar ratio in the scaffold was measured at 3.19, which is higher than the stoichiometric value. This elevated ratio is commonly observed in composite scaffolds due to the masking or partial attenuation of the phosphorus peak by polymeric components, particularly during EDX quantification, which tends to overestimate calcium and underestimate phosphorus in the presence of organic matrices. In this case, the presence of PCL and gelatin reduced the detectable phosphate signals, resulting in a higher apparent Ca/P ratio. Similar findings have been reported in recent studies, where polymer-coated or polymer-reinforced hydroxyapatite composites exhibited Ca/P ratios exceeding the stoichiometric value, not due to chemical degradation of HA, but due to limitations of EDX in accurately detecting light elements and buried phosphate groups beneath organic phases (Shahzamani et al., 2022).

Table 2. Elemental Composition of Scaffold CHAp/PCL/Gelatin Based on EDX Analysis

Element	Weight %	Atomic %
Ca	13.07	4.79
P	3.16	1.50
O	20.79	19.09
C	49.97	61.14

3.4 Mechanical Testing (Compressive Strength)

The compressive strength of the CHAp/PCL/Gelatin scaffold was measured at 2.693 MPa, which falls within the range of trabecular bone (2–12 MPa) (Gibson & Ashby, 1997). The combination of CHAp with PCL and gelatin enhanced the mechanical stability compared to gelatin-based scaffolds alone, while maintaining suitable porosity. The incorporation of PCL contributed to increased strength due to its semi-crystalline structure and high modulus, whereas gelatin improved hydrophilicity, aiding cell attachment.

Table 3. Compressive strength values of CHAp/PCL/Gelatin scaffold

Repetition	Sample	Compressive Strength (MPa)
1	Scaffold CHAp/PCL/Gelatin	2.287
2	Scaffold CHAp/PCL/Gelatin	2.833
3	Scaffold CHAp/PCL/Gelatin	2.960
Mean		2.693

As shown in **Table 3**, the CHAp/PCL/Gelatin scaffold achieved a compressive strength of 2.693 MPa, placing it at the lower-mid range of natural trabecular bone (2–12 MPa) (Nugroho et al., 2022). This value suggests that the scaffold can withstand physiological stresses typical of cancellous bone regions while maintaining sufficient porosity for tissue ingrowth. Compared to pure CHAp scaffolds reported in previous studies, which typically exhibit compressive strength below 2 MPa (El-Fattah et al., 2021). The mechanical properties, moderately higher, likely due

to the reinforcing effect of PCL's semi-crystalline matrix. Gelatin, although not contributing significantly to strength, enhances the material's capacity to interact with cells by improving surface hydrophilicity. The balance between mechanical performance and porosity indicates that the scaffold is mechanically competent while still promoting biological integration.

3.5 Biodegradation Test

Biodegradation testing revealed a weight loss of approximately 3% after 24 hours of immersion in PBS at 37 °C. This rate of initial mass loss is considered ideal for the early stage of scaffold implantation, allowing gradual replacement by newly formed bone tissue (Wang et al., 2024). The degradation behavior was influenced by the hydrophilicity of gelatin, which facilitated water absorption, and the crystalline nature of PCL, which slowed degradation. The presence of carbonate substitution in CHAp may have further enhanced its dissolution in the physiological environment, as widely reported for B-type CHAp in recent studies (Zhou et al., 2023).

Table 4. Weight loss percentage of CHAp/PCL/Gelatin scaffold after 24 hours in PBS.

Repetition	Sample	Initial Weight	Final Weight	% Weight Loss
1	Scaffold CHAp/PCL/Gelatin	0.4936	0.4788	3.006%
2	Scaffold CHAp/PCL/Gelatin	0.4880	0.4734	2.999%
3	Scaffold CHAp/PCL/Gelatin	0.5158	0.5003	3.008%
	Mean	0.4991	0.4842	3.004%
	Standard Deviation	±0.0143	±0.0139	±0.0045%

As shown in **Table 4**, the CHAp/PCL/Gelatin scaffold exhibited an average weight loss of approximately 3%. The degradation behavior can be explained by the hydrophilicity of gelatin, which accelerates water uptake and initiates early mass loss, since gelatin absorbs fluid rapidly due to its polar functional groups (Hussain et al., 2023). In addition, the carbonate substitution in CHAp increases its solubility under physiological conditions, leading to faster ionic exchange and partial mineral dissolution (Zhou et al., 2022). Conversely, PCL possesses a hydrophobic and semi-crystalline structure, acting as a physical barrier that limits water penetration and slows the overall degradation rate of the scaffold (Kumar et al., 2022). This complementary degradation mechanism ensures a controlled resorption profile, maintaining scaffold stability while still supporting gradual tissue ingrowth and regeneration.

4. Conclusions

This study successfully synthesized B-type carbonated hydroxyapatite (CHAp) from *Nucella lamellosa* shells using a precipitation method followed by sintering at 600 °C. The CHAp/PCL/Gelatin scaffold fabricated via the freeze-drying method exhibited interconnected pores with an average diameter of 28.94 µm, a compressive strength of 2.693 MPa, and an initial biodegradation rate of 3% after 24 hours. XRD and FTIR analyses confirmed the presence of CHAp in the composite and successful incorporation of PCL and gelatin without altering its functional groups. The XRD confirmed the presence of CHAp by showing diffraction peaks that matched the characteristic planes of hydroxyapatite, while FTIR validated the successful incorporation of PCL and gelatin through the detection of their specific functional groups without the disappearance of CHAp's phosphate and carbonate bands. The reduced crystallinity (37.29%) in the scaffold compared to pure CHAp is expected to enhance bioactivity and degradation behavior. Furthermore, the pore morphology (SEM), mechanical strength (compression test), and biodegradation profile collectively indicate that the scaffold meets the structural, mechanical, and degradation criteria required for bone tissue engineering applications.

5. Bibliography

- Ahmed, E. M., Abdel-Mohsen, A. M., & Hassan, E. A. (2022). Biodegradable polymeric scaffolds for bone tissue engineering applications. *Journal of Polymers and the Environment*, 30(1), 120–135. <https://doi.org/10.1007/s10924-021-02182-2>
- Cieza, A., Causey, K., Kamenov, K., Hanson, S. W., Chatterji, S., & Vos, T. (2021). Global estimates of the need for rehabilitation based on the Global Burden of Disease study 2019. *The Lancet*, 396(10267), 2006–2017. [https://doi.org/10.1016/S0140-6736\(20\)32340-0](https://doi.org/10.1016/S0140-6736(20)32340-0)
- Ebrahimi, M., et al. (2022). Carbonated hydroxyapatite-based scaffolds for bone regeneration. *Ceramics International*, 48(12), 18123–18135. <https://doi.org/10.1016/j.ceramint.2022.03.129>
- El-Fattah, A. A., et al. (2021). Structural and biological evaluation of hydroxyapatite-based composites for biomedical applications. *Materials Science and Engineering C*, 120, 111698. <https://doi.org/10.1016/j.msec.2020.111698>
- Figueiredo, M., Cunha, S., Martins, J., & Lopes, M. (2021). Influence of surface morphology of hydroxyapatite on cell behavior. *Materials Today: Proceedings*, 45, 4534–4538. <https://doi.org/10.1016/j.matpr.2020.09.707>
- Gibson, L. J., & Ashby, M. F. (1997). *Cellular solids: Structure and properties* (2nd ed.). Cambridge University Press.
- Hernandez, C. J., & Woodrow, K. A. (2024). Trends in biomaterials for bone regeneration: Challenges and future

- perspectives. *Advanced Healthcare Materials*, 13(2), 2301215. <https://doi.org/10.1002/adhm.202301215>
- Hussain, A., et al. (2023). Hydrophilicity-driven scaffold degradation for tissue engineering. *Journal of Biomedical Materials Research Part A*, 111(5), 928–939. <https://doi.org/10.1002/jbm.a.37628>
- Ielo, I., et al. (2022). Recent advances in hydroxyapatite-based biocomposites for bone tissue engineering. *Materials Science and Engineering C*, 130, 112469. <https://doi.org/10.1016/j.msec.2021.112469>
- Lee, S. S., et al. (2022). Scaffolds for bone tissue engineering: Advances and future trends. *Materials Today Bio*, 13, 100174. <https://doi.org/10.1016/j.mtbio.2021.100174>
- Li, X., et al. (2021). Hydroxyapatite composites for bone regeneration: Structure, properties, and applications. *Composites Part B: Engineering*, 224, 109152. <https://doi.org/10.1016/j.compositesb.2021.109152>
- Liu, Y., et al. (2022). Nanostructured hydroxyapatite for improved bioactivity in bone repair. *Journal of Asian Ceramic Societies*, 10(3), 563–572. <https://doi.org/10.1080/21870764.2022.2034421>
- Martins, J., et al. (2023). Carbonated hydroxyapatite scaffolds: Recent insights and biomedical applications. *Journal of Biomedical Materials Research Part B*, 111(1), 75–87. <https://doi.org/10.1002/jbm.b.35194>
- Min, K. H., et al. (2024). Biomimetic calcium-based scaffolds for bone tissue engineering. *Materials Science and Engineering C*, 143, 115655. <https://doi.org/10.1016/j.msec.2023.115655>
- Nguyen, T., et al. (2022). Mechanical evaluation of hydroxyapatite–polymer scaffolds for bone tissue engineering. *Polymer Testing*, 113, 107665. <https://doi.org/10.1016/j.polymertesting.2022.107665>
- Nugroho, A., et al. (2022). Characterization of bioceramic-based scaffolds from natural precursors. *Journal of Biomaterials Applications*, 37(1), 33–45. <https://doi.org/10.1177/08853282221084633>
- Permatasari, D., et al. (2021). Hydroxyapatite from natural resources for biomedical applications. *Materials Today: Proceedings*, 44, 3149–3154. <https://doi.org/10.1016/j.matpr.2020.11.413>
- Rahman, M. M., et al. (2021). Influence of pore structure on the biodegradation of bone scaffolds. *Journal of Applied Biomaterials & Functional Materials*, 19, 1–10. <https://doi.org/10.1177/22808000211021234>
- Rahman, M. S., et al. (2023). Controlled degradation behavior of polymer–ceramic scaffolds. *International Journal of Biological Macromolecules*, 232, 124713. <https://doi.org/10.1016/j.ijbiomac.2023.124713>
- Shahzamani, M., et al. (2022). Hydroxyapatite-based nanomaterials for bone regeneration: A review. *Journal of Drug Delivery Science and Technology*, 74, 103553. <https://doi.org/10.1016/j.jddst.2022.103553>
- Sun, X., et al. (2022). Carbonated hydroxyapatite scaffolds with enhanced bioactivity. *Ceramics International*, 48(14), 20123–20132. <https://doi.org/10.1016/j.ceramint.2022.04.137>
- Todd, N. M., et al. (2024). Functional scaffolds for bone tissue regeneration: Design considerations and applications. *Biomaterials Advances*, 162, 213571. <https://doi.org/10.1016/j.bioadv.2023.213571>
- Wang, Y., et al. (2024). Effect of carbonate substitution on hydroxyapatite dissolution in physiological environments. *Journal of the European Ceramic Society*, 44(5), 2451–2460. <https://doi.org/10.1016/j.jeurceramsoc.2023.12.015>
- World Health Organization. (2021). *Global status report on road safety*. <https://www.who.int>
- Zhang, L., et al. (2020). Polymer–ceramic composite scaffolds for bone repair. *Composites Science and Technology*, 199, 108364. <https://doi.org/10.1016/j.compscitech.2020.108364>
- Zhou, H., et al. (2022). Effect of crystallinity on the biodegradation behavior of hydroxyapatite-based scaffolds. *Materials Chemistry and Physics*, 287, 126273. <https://doi.org/10.1016/j.matchemphys.2022.126273>
- Zhou, Y., et al. (2023). Carbonated hydroxyapatite: Structure, dissolution, and biomedical relevance. *Progress in Biomaterials*, 12, 255–269. <https://doi.org/10.1186/s40204-023-00187-5>